stellarator news

Published by Fusion Energy Division, Oak Ridge National Laboratory
Building 5700 P.O. Box 2008 Oak Ridge, TN 37831-6169, USA

Editor: James A. Rome Issue 114 April 2008
E-Mail: jar@ornl.gov Phone (865) 482-5643

On the Web at *http://www.ornl.gov/sci/fed/stelnews*

Wendelstein 7-X newsletter available

The first issue of a newsletter on the Wendelstein 7-X project has been launched by the Max-Planck-Institut für Plasmaphysik, Greifswald, Germany. The newsletter is scheduled to be available on the Web about four times a year:

German: http://www.ipp.mpg.de/ippcms/de/for/publikationen/w7xletters/
English: http://www.ipp.mpg.de/ippcms/eng/for/publikationen/w7xletters/

Wendelstein 7-X

NEWSLETTER

No. 1 / April 2008

First major milestone achieved

The first two half modules of Wendelstein 7-X have left their assembly stands and have been moved to the next stand for joining them together to a whole module. The next assembly steps will include the installation of the superconducting bus and the cryo-piping, connecting the coils to power and liquid helium supplies. In parallel the assembly of the second pair of half-modules will be started.

Initially hampered by quality problems, in particular with the electrical insulation of the super-conducting coils, and requiring considerable additional engineering efforts to improve the coil support structure, the assembly proper of the device finally started mid 2007 and since then proceeded without delays.

A completed half module on its way to the next assembly stand

Fig. 1. The Wendelstein 7-X Newsletter as available online.

Persons interested in subscribing to the newsletter may contact Dr. Andreas Dinklage at w7xnewsletter@ipp.mpg.de.

The content of the first issue is also given in the following article.

In this issue . . .

All opinions expressed herein are those of the authors and should not be reproduced, quoted in publications, or used as a reference without the author's consent.
Oak Ridge National Laboratory is managed by UT-Battelle, LLC, for the U.S. Department of Energy.

Wendelstein 7-X achieved major assembly milestone

The first two half modules of Wendelstein 7-X have left their assembly stands and have been moved to the next stand for joining them together to create a whole module. The next assembly steps will include the installation of the superconducting bus and the cryo-piping that connect the coils to the power and liquid helium supplies. In parallel the assembly of the second pair of half-modules will be started.

Initially construction was hampered by quality problems. In particular, there were issues with the electrical insulation of the superconducting coils, which required considerable additional engineering efforts to improve the coil support structure. The assembly proper of the device finally started in mid-2007 and since then has proceeded without delays.

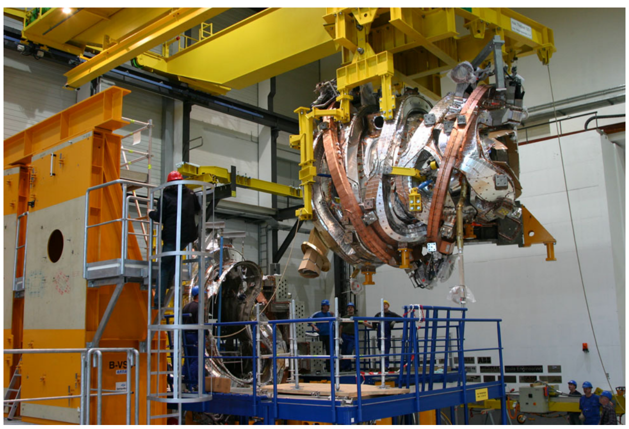

Fig. 2. A completed half-module on its way to the next assembly stand (photo: Beate Kemnitz, IPP).

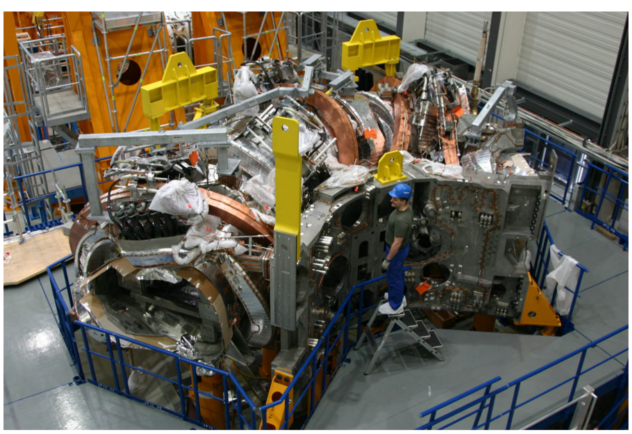

Fig. 3. The two half-modules in assembly stand II (photo: Antje Richter, IPP).

By now the assembly progress is no longer determined by the delivery of the coils—all 70 superconducting coils have been manufactured. Altogether, about half of the coils have successfully passed cryo and high-voltage tests.

After a revision of the assembly schedule and a reorientation of the start-up requirements of Wendelstein 7-X, the completion of the assembly is now foreseen for 2014. The main measures to achieve this completion date are intensified shift work, the omission of 45 ports, and a start-up configuration without actively cooled in-vessel components. Although in the long run the omission of ports may reduce the experimental flexibility, none of the scientific objectives of Wendelstein 7-X will be affected.

During the first two years of plasma operation, without active cooling, high power operation of up to 8–10 MW will be limited to 5–10 s. The available heating systems will be either 8 MW of electron cyclotron resonance heating, already prepared for steady-state operation, or 7 MW of neutral beam injection, resulting in a total of about 11 MW limited by the power supplies. At a 1 MW power level, discharge durations of about 50 s will be possible. First experiments will focus on preparing for the later steady-state operation by verifying the divertor heat load distribution, on demonstrating improved neoclassical confinement in the low mean free path regime, and on first attempts to develop an integrated high-density, improved confinement regime.

This initial phase will be followed by a 18-month shutdown for upgrading Wendelstein 7-X to its full steady-state capability. This includes in particular the installation of an actively cooled divertor for heat fluxes of up to 10 MW/m^2.

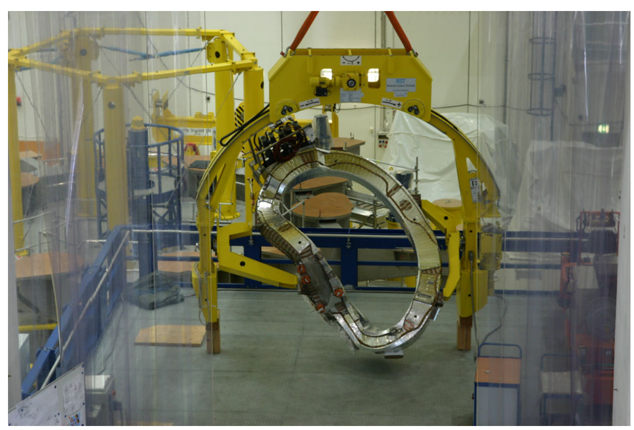

Fig. 4. The next nonplanar coil is waiting for assembly (photo: Antje Richter, IPP).

W7-X Newsletter
Coordination: Prof. a. D. Dr. Robert Wolf
Contact: Dr. Andreas Dinklage
E-mail: andreas.dinklage@ipp.mpg.de

Wendelstein 7-AS review published

The review "Major Results from the Stellarator Wendelstein 7 -AS" has now been published online by *Plasma Physics and Controlled Fusion* at http://www.iop.org/EJ/journal/-page=featured/0741-3335. The printed version will appear in the May issue.

Wendelstein 7-AS (W7-AS) was the first stellarator device that used modular field coils instead of large helical windings. The successful operation proved that three-dimensional (3D) magnetic field configurations with flux surfaces of high quality can be produced by modular coils. Thus this concept provides the technical basis for building optimized stellarators, which use modular coils. W7-AS was the first step to test some of the basic elements of stellarator optimization, and it showed that essential optimization criteria can be met simultaneously, namely:

An improved equilibrium with reduced Shafranov shift and improved stability properties resulted in β values up to 3.4% (at 0.9 T). The magnitude of the observed Shafranov shift as well as its dependence on the rotational transform are consistent with predictions. The β limit was determined by power balance and impurity radiation without noticeable degradation of stability or a violent collapse. Of important operational value are the slow time scales of the plasma decay and the absence of current-driven instabilities close to the operational boundaries at the density and β limits.

A partial reduction of neoclassical transport in the plateau regime was achieved by an average elongation of the flux surfaces and beyond this by the neoclassical impact of the radial electric field. For high core temperatures, neoclassical transport with its strongly rising temperature dependence prevails. For these conditions, the experimental results were in good agreement with calculations confirming the reliability of neoclassical predictions and the feasibility of the concept of drift optimization. A full neoclassical optimization was beyond the scope of this project. Because of this the bootstrap current was still "tokamak-like" and no design effort has been made to reduce it by further optimization, but the measurements agree well with the expectations, giving confidence in the desired minimization of the bootstrap current in W7-X.

The energy confinement was about a factor of 2 above ISS95 without degradation near operational boundaries. A number of improved confinement regimes, such as core electron-root confinement with central $T_e \leq 7\,\mathrm{keV}$ and regimes with strongly sheared radial electric field at the plasma edge resulting in $T_i \leq 1.7\,\mathrm{keV}$, were obtained. W7-AS is the first non-tokamak device to have achieved the H-mode and moreover developed a high density H-mode (HDH) regime with strongly reduced impurity confinement that allowed quasi steady-state operation ($\tau \approx 65\tau_E$) at 2.5 T and densities $\bar{n}_e \cong 4 \times 10^{20}\,\mathrm{m}^{-3}$ (exceeding the Greenwald limit of an equivalent tokamak by a factor of 2.5) under demanding conditions ($\beta > 3\%$, $\tau_p/\tau_E = 2$).

A variety of non-ohmic heating and current drive scenarios by ICRH, NBI, and, in particular, ECRH were tested and compared successfully with theoretical predictions. In order to explore the stellarator-specific high-density path to a reactor regime, new heating schemes for overdense plasmas were developed, such as RF mode conversion heating—Ordinary mode, Extraordinary mode, Bernstein-wave (OXB) heating—or second harmonic O-mode (O2) heating.

For the first time in a helical system, a modular island divertor was tested, with applicability to W7-X and conceptually to a stellarator reactor. The divertor was operated with stable partial detachment, in agreement with numerical simulations.

W7-AS laid the physics background for operation of an optimized low-shear steady-state stellarator, but its complementary characteristics also have helped to better understand the tokamak. This applies to the differences in field structure, e.g., low global shear or strong toroidal viscosity; to features of the H-mode, e.g., the existence of iota windows or the role of the neoclassical electric field at the plasma edge; to the spectrum of Alfvén waves under strong shaping; to the bootstrap current, which can be much more easily measured without inductive background; to the boundary-layer and divertor physics with 3D effects e.g., with local limiters or ergodic boundary layers at the tokamak edge; and to the physics of operational limits—those subject to MHD or power balance. This list could be extended.

W7-AS ceased operation mid-2002 (Fig. 1). The continuation of the experimental stellarator work of IPP is expected by 2014. This gap reflects the step from a laboratory-based experiment, W7-AS, to the superconducting steady-state system W7-X, with fabrication and assembly complexity and the challenge of high-performance operation requiring a completely actively cooled first wall, divertor, and in-vessel components. Fusion power plants must operate in steady state; this demand is imposed by material aspects, by their large power to the grid, and possibly by competitive considerations with regard to the next generation of fission reactors (Generation IV). The choices in fusion are either 3D systems with increased mechanical complexity but benign operational characteristics or 2D systems with higher operational complexity. The performance of W7-AS has shown that optimized stellarators are an option with high potential.

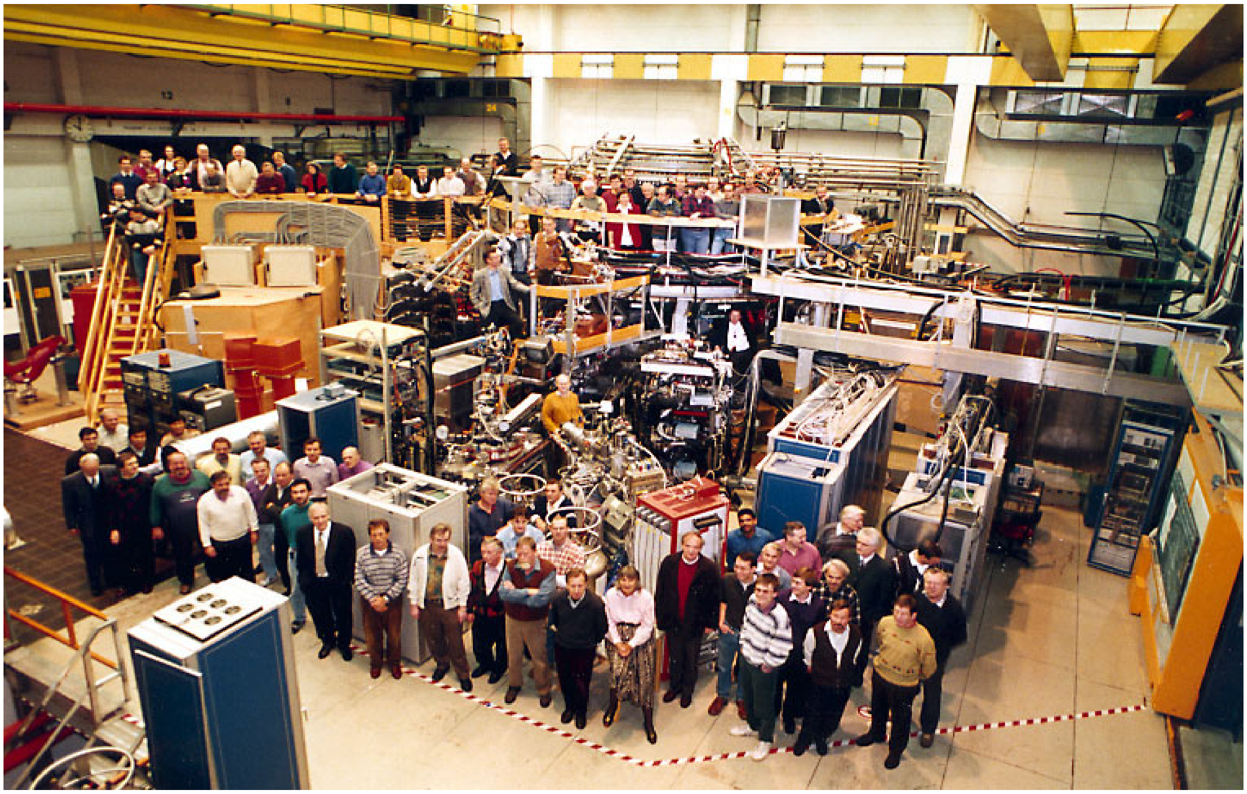

Fig. 1. The W7-AS Team in the experiment hall at the final shutdown in July 2002.

Matthias Hirsch for the Wendelstein Team
Division W7-X Physics
Max-Planck-Institut für Plasmaphysik
D-17491 Greifswald, Germany
E-mail: Matthias.Hirsch@ipp.mpg.de

Evidence of long-distance correlation of fluctuations during edge transitions to improved confinement regimes in the TJ-II stellarator

First- and second-order phase transition models with ***E***×***B*** sheared flow as a key ingredient have been invoked to explain the transition to improved confinement regimes [1–4]. Zonal flows have also been suggested as an important ingredient to explain the Low to High (L-H) transition in magnetic confinement devices [5, 6 and references therein]. In the framework of the physics of second-order phase transition, the correlation length of fluctuations and the relaxation time (in the order parameter) are expected to diverge at the transition point. Thus, the development of edge plasma diagnostics to characterize the emergence of sheared flows and to quantify the degree of long-range correlation can provide relevant information on mechanisms involved in the transition to improved confinement regimes.

In the TJ-II stellarator, sheared flows can be easily driven and damped at the plasma edge by changing the plasma density [7, 8] or during biasing experiments [9]. The experimental results on the emergence of the shear flow layer in TJ-II have some of the characteristics of a transition and are consistent with the expectations of second-order transition models of turbulence-driven sheared flows [3]. In particular, measurements of the relaxation time of externally induced electric fields show that an increase above the threshold gradient triggers the development of sheared flows, in agreement with the model [10]. The recent development of two sets of Langmuir probes located at two toroidal positions in the TJ-II stellarator makes this device an excellent laboratory for investigating long-distance correlations during the transition to improved confinement regimes.

Experiments were carried out in the TJ-II stellarator in electron cyclotron resonance heated plasmas ($P_{\mathrm{ECRH}} \leq$ 400 kW, $B_{\mathrm{T}} = 1$ T, $\langle R \rangle = 1.5$ m, $\langle a \rangle \leq 0.22$ m, $\iota(a)/2\pi \approx$ 1.5–1.9). The plasma density was modified in the range $(0.35–1) \times 10^{19}$ m^{-3}. Different edge plasma parameters were simultaneously characterized at two toroidal positions approximately 160º apart using two similar multi-Langmuir probes, installed on fast reciprocating drives (approximately 1 m/s) [11]. The arrangement of both probes in TJ-II is illustrated in Fig. 1.

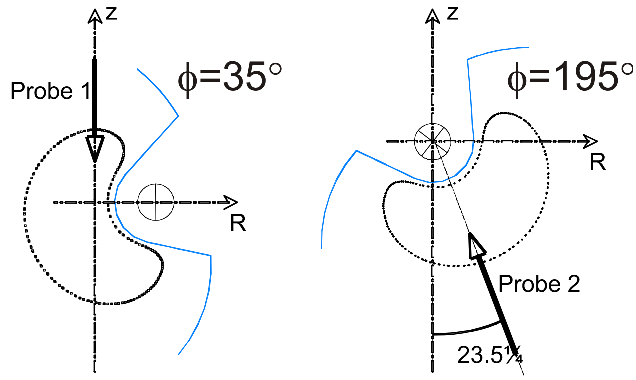

Fig. 1. Schematic view of the locations of the two probes (thick arrows) and their positions relative to the TJ-II plasma.

One of the probes (Probe 1) is located in a top window entering vertically through one of the “corners” of its beam-shaped plasma and at $\phi = 35$º (where ϕ is the toroidal angle in the TJ-II reference system). Probe 2 is installed in a bottom window at $\phi = 195$º and enters the plasma through a region with a higher density of flux surfaces (i.e., lower flux expansion) than Probe 1. Note that the field line passing through one of the probes is approximately 150º poloidally displaced when reaching the toroidal position of the other probe, which is more than 5 m away. A graphite electrode (12 mm high, 25 mm diam) was developed for biasing experiments on TJ-II and has proved to be a valuable tool for controlling the edge plasma electric field and consequently for placing the plasma in an enhanced confinement regime. Edge radial profiles of different plasma parameters have been measured simultaneously at the two separate toroidal locations.

The development of sheared flows at the plasma edge of the TJ-II requires a critical value of plasma density or density gradient that depends on global plasma parameters [12]. Fast imaging of the plasma edge in shots with different values of density also revealed an effect of the shear layer on turbulent structures, in good agreement with probe results [13].

The perpendicular electric field fluctuations (i.e., the turbulent radial velocity $\tilde{v}_r = \tilde{E}_\theta / B$) and the perpendicular phase velocity measured at the plasma edge as a function of plasma density are shown in Fig. 2. Measurements have been obtained simultaneously with both probe systems, located at approximately the same radial position ($\rho = r/a \approx 0.9$), while changing density from shot to shot. The fluctuation levels and the turbulent transport increase as density increases to the critical value for which sheared flows are developed. For densities above the threshold, and once sheared flows are fully developed, the fluctuation level and the turbulent transport slightly decreases and the edge gradients become steeper. Edge sheared flows are developed at the same threshold density in the two toroidal positions.

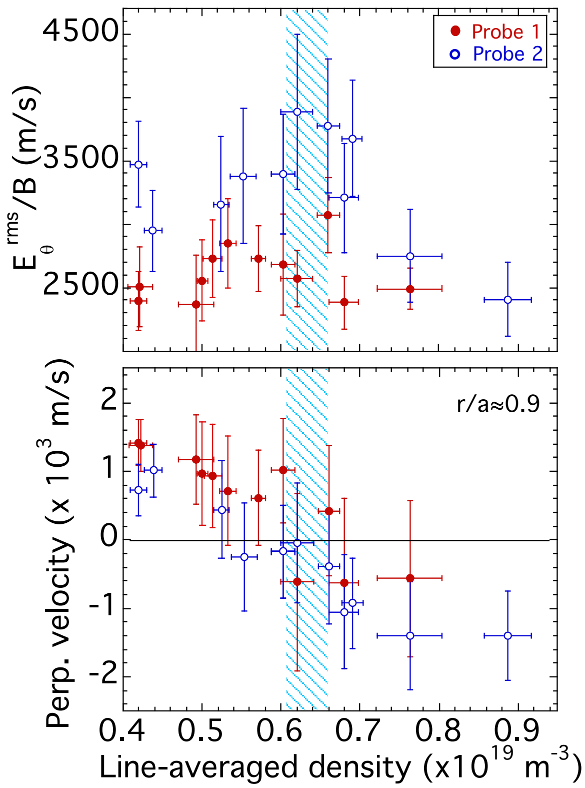

Fig. 2. Averaged electric field fluctuations and perpendicular velocity measured at two toroidal locations and at approximately the same radial position (ρ/a ~ 0.9) as a function of plasma density.

The development of edge sheared flows has also been induced in TJ-II using an electrode that externally imposes a radial electric field at the plasma edge. The response of the plasma to biasing is different at densities below and above the threshold value needed to trigger the spontaneous development of $\boldsymbol{E}\times\boldsymbol{B}$ sheared flows [9], but it is similar at the two toroidal locations.

Floating potential signals measured at both toroidal locations show a striking similarity mainly for low-frequency components, contrary to that observed in the ion saturation current signals. This similarity is observed at different time scales, but it is more clear during fluctuation events with time scales in the range of 0.1–1 ms related to the shear flow development [10]. To quantify the similarity between probe signals, the toroidal cross-correlation has been computed for a wide range of TJ-II plasma conditions, including a line-averaged density scan as well as with and without electrode bias in plasmas without MHD activity as shown by the pick-up coils installed in TJ-II.

The toroidal cross-correlation of the floating potential and the ion saturation current signals measured at different radial positions of Probe 1 while Probe 2 is fixed at ρ/a ~ 0.95 is shown in Fig. 3 with and without biasing, for ECRH plasmas and with similar line-averaged density ($n_e \approx 0.65 \times 10^{19}$ m^{-3}), close to the critical value. The ion saturation current toroidal correlation is very low in agreement with previous measurements of the parallel correlation in the scrape-off layer (SOL) region that have shown an increase of correlation only when probes were located at the same field line [14, 15]. However, the correlation between floating potential signals is significant, particularly during biasing when it increases while the ion saturation current correlation is in the noise level range. The maximum floating potential correlation is observed when the probes are approximately at the same radial location. The toroidal correlation shows a maximum in the region just inside the LCFS, both with and without bias, being negligible near the SOL.

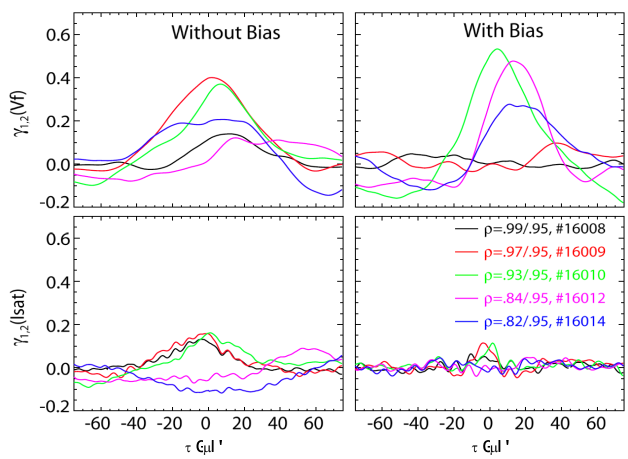

Fig. 3. Cross-correlation function for floating potential and ion saturation current signals measured at different radial positions of probe 1 (while probe 2 is fixed) with and without biasing in ECRH plasmas with similar line-averaged density ($n_e \approx 0.65 \times 10^{19}$ m^{-3}) in both regimes.

Figure 4 illustrates the dependence of the toroidal floating potential correlation on the line-averaged density (for the same shots presented in Fig. 2). It is observed that the cross-correlation depends on the density, being larger as density increases to $n_e \approx 0.6 \times 10^{19}$ m^{-3}, which corresponds to the threshold density for shear flow development for the selected plasma configuration (see Fig. 2). Although experimentally the external control used is the plasma line-averaged density, the local plasma parameters (i.e., ion saturation current gradient) should be used as a more suitable control parameter [3]. The increase of correlation with density results mainly from the rise in the correlation at low frequencies (below 20 kHz).

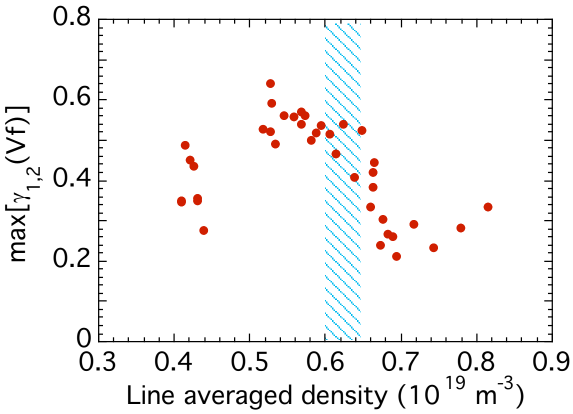

Fig. 4. Maximum value of the cross-correlation function between floating potential signals measured at approximately the same radial positions of both probes (ρ/a ~ 0.9) as a function of plasma density. Shadowed area indicates the critical density region.

Figure 5 shows the time evolution of plasma density and the cross-correlation between ion saturation current and floating potential signals (measured by Probes 1 and 2). It shows clearly the increase in the floating potential cross-correlation during the biasing phase, with a time delay for the maximum cross-correlation in the range of 5–10 μs in the different scenarios, as the radial electric field (and so the sheared flows) develop first at Probe 2, rather than at Probe 1. On the contrary, the degree of long-range correlation is negligible in density fluctuations (as shown in Fig. 3). Note that in the biasing experiments reported in Fig. 5, the plasma density is below the critical value in the phase without biasing ($t < 100$ ms), exceeding the critical value during the biasing phase ($100 < t < 150$ ms). Once the biasing is turned off, the density decreases on the time scale of the particle confinement time (in the range of 10 ms), whereas both the electric field and the degree of long-range correlation decrease in a much faster time scale. These results show that the high degree of long-range correlation observed in floating potential signals is coupled to the value of radial electric field and not to the plasma density.

In conclusion, TJ-II results show the importance of long-distance correlation as a first step in the transition to improved confinement regimes and the key role of electric fields to amplify them. The present findings point out the important role of edge diagnostic development to characterize simultaneously at different plasma locations the structure of sheared flows and fluctuations to unravel of physics of sheared flows. Comparative studies stellarator - tokamak (during L-H transition) should be stimulated to provide a critical test for the L-H transition physics mechanisms.

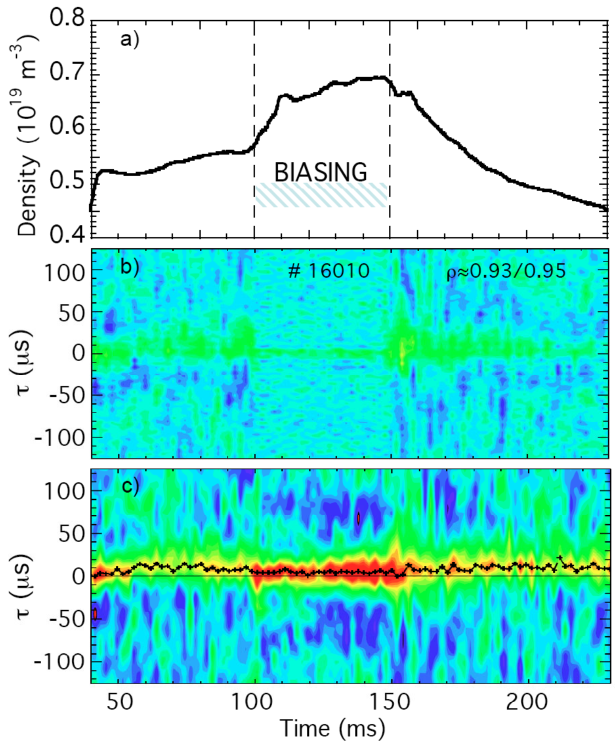

Fig. 5. Delay of cross-correlation function between (b) ion saturation current and (c) floating potential signals measured toroidally apart and at the plasma edge as a function of time for one shot during biasing experiments. The overplotted solid line in (c) represents the evolution of the time delay where the correlation is maxima. Line averaged density for the same shot is also shown (a).

M. A. Pedrosa, C. Hidalgo, D. Carralero and C. Silva*
EURATOM-CIEMAT (Spain) and * EURATOM-IST (Portugal)
E-mail: angeles.pedrosa@ciemat.es

References

[1] P. W. Terry, Rev. Mod. Phys. **72** (2000) 109.

[2] P. Diamond et al., Phy. Rev. Lett. **72** (1994) 2565.

[3] B. A. Carreras et al., Phys. Plasmas **13** (2006) 122509.

[4] P. Mantica et al., Phys. Rev. Lett. **96** (2006) 095002.

[5] P. N. Guzdar et al., Phys. Rev. Lett. **87** (2001) 015001.

[6] P. H. Diamond et al., Plasma Phys. Control. Fusion **47** (2005) R35.

[7] C. Hidalgo, M. A. Pedrosa, L. Garcia, and A. Ware, Phys. Rev. E **70** (2004) 067402.

[8] M. A. Pedrosa et al., Plasma Phys. Control. Fusion **47** (2005) 777.

[9] C. Silva et al., Czech. J. Phys. **55** (2005) 1589.

[10] M. A. Pedrosa et al., Plasma Phys. Control. Fusion **49** (2007) B303.

[11] M. A. Pedrosa, et al., Rev. Sci. Instrum. **70** (1999) 415.

[12] M. A. Pedrosa, C. Hidalgo, et al., Czech. J. Phys. **55** (2005) 1579.

[13] J. A. Alonso et al., Plasma Phys. Control. Fusion **48** (2006) B465.

[14] Ch. P. Ritz et al., Rev. Sci. Instrum. **59** (1988) 1739.

[15] H. Thomsen et al., Phys. Plasmas **9** (2002) 1233.